Proceedings of the 5th WSEAS/IASME Int. Conf. on SYSTEMS THEORY and SCIENTIFIC COMPUTATION, Malta, September 15-17, 2005 (pp139-144)

An Accurate High-order Validated Method to Solve the 3D Laplace Equation

M.L.SHASHIKANT, MARTIN BERZ and KYOKO MAKINO
Department of Physics and Astronomy
Michigan State University
East Lansing, MI 48824
USA
manikond@msu.edu, berz@msu.edu, makino@msu.edu http://bt.pa.msu.edu/

Abstract: The 3D Laplace equation is one of the important PDEs of Physics, describing among others the phenomenology of electrostatics and magnetostatics. For various practical problems, very precise and validated solutions of this PDE are required; but with conventional finite element or finite difference codes this is difficult to achieve even without validation because of the need for an exceedingly fine mesh which leads to often prohibitive CPU time. We present an alternative approach based on high-order quadrature and a high-order finite element method. Both of the ingredients become accessible through the use of Taylor model methods. The solution in space is first represented as a Helmholtz integral over the two-dimensional surface. The latter is executed by evaluating the kernel of the integral as a Taylor model of both the two surface variables and the three volume variables inside the cell of interest. Finally, the integration over the surface variables is executed as a mere polynomial integration, resulting in a local Taylor model of the solution within one cell. Examples of the method and the precision that can be achieved will be given.

Key-Words: Taylor model, COSY INFINITY, PDE solver, Helmholtz method, differential algebra, interval arithmetic.

1 Introduction

Many problems in physics and engineering require the solution of the three dimensional ($3D$) Laplace equation

$$\Delta\psi\left(\overrightarrow{r}\right) = 0 \text{ in the bounded volume } \Omega \subset \mathtt{R}^3 \quad (1)$$

It is well known that under mild smoothness conditions for the boundary $\partial\Omega$ of Ω, the Laplace equation admits unique solutions if either ψ or its derivative normal to $\partial\Omega$ are specified on the entire boundary surface $\partial\Omega$. In many typical applications, not only the normal derivative of ψ but indeed the entire gradient $\vec{\nabla}\psi$ is known on the surface; for example, in the magnetostatic case the entire field $\vec{B} = \vec{\nabla}\psi$ is measured, and not merely whatever component happens to be normal to the surface under consideration. The corresponding problem of determining ψ based on the knowledge of the field $\vec{\nabla}\psi\left(\overrightarrow{r}\right) = \overrightarrow{f}\left(\overrightarrow{r}\right)$ on the surface $\partial\Omega$ is referred to as the Helmholtz problem.

Analytic closed form solutions for the 3D case can usually only be found for special problems with certain regular geometries where a separation of variables can be performed. However, in most practical 3D cases, numerical methods are the only way to proceed. Frequently the finite difference or finite element approaches are used to find the approximations of the solution on a set of points in the region of interest. But because of their relatively low approximation order, for the problem of precise solution of PDEs, the methods have very limited success because of the prohibitively large number of mesh points required. For reference, codes like the frequently used TOSCA [1, 2] can usually solve 3D Laplace problems with a relative accuracy of 10^{-4} with meshes of size about 10^{-6}[18]. Furthermore, direct validation of such methods is often very difficult.

In the following we develop a new method based on the Helmholtz theorem and the Taylor model methods[10, 9] and the corresponding tools in the code COSY Infinity [4, 6] to find a validated solution of the Laplace equation starting from the field boundary data. The final solution is provided as a set of local Taylor models, each of which represents an enclosure of a solution for a sub-box of the volume of interest.

2 Theory and Implementation

2.1 The Helmholtz Approach

We begin by representing the solution of the Laplace equation via the Helmholtz vector decomposition theorem [11, 12, 14, 17, 15, 16], which states that any vector field $\overrightarrow{B}$ which vanishes at infinity can inside an arbitrary boundary region Ω be written as the sum of two terms

$$\overrightarrow{B}\left(\vec{x}\right) = \vec{\nabla} \times \vec{A}_t\left(\vec{x}\right) + \vec{\nabla}\phi_n\left(\vec{x}\right), \qquad (2)$$

where

$$\begin{aligned}\phi_n\left(\vec{x}\right) =& \frac{1}{4\pi}\int_{\partial\Omega} \frac{\vec{n}\left(\vec{x}_s\right)\cdot\overrightarrow{B}\left(\vec{x}_s\right)}{\left|\vec{x}-\vec{x}_s\right|}ds \\ &- \frac{1}{4\pi}\int_{\Omega} \frac{\vec{\nabla}\cdot\overrightarrow{B}\left(\vec{x}_v\right)}{\left|\vec{x}-\vec{x}_v\right|}dV \\ \vec{A}_t\left(\vec{x}\right) =& -\frac{1}{4\pi}\int_{\partial\Omega} \frac{\vec{n}\left(\vec{x}_s\right)\times\overrightarrow{B}\left(\vec{x}_s\right)}{\left|\vec{x}-\vec{x}_s\right|}ds \\ &+ \frac{1}{4\pi}\int_{\Omega} \frac{\vec{\nabla}\times\overrightarrow{B}\left(\vec{x}_v\right)}{\left|\vec{x}-\vec{x}_v\right|}dV.\end{aligned}$$

Here $\partial\Omega$ is the surface which bounds the volume Ω. $\vec{x}_s$ denotes points on the surface $\partial\Omega$, and $\vec{x}_v$ denotes points within Ω. $\vec{n}$ is the unit vector perpendicular to $\partial\Omega$ that points away from Ω, and $\vec{\nabla}$ denotes the gradient with respect to $\vec{x}_v$.

The first term is usually referred to as the solenoidal term, and the second term as the irrotational term. Because of the apparent similarity of these two terms to the well-known vector- and scalar potentials to $\vec{B}$, we note that in the above representation, it is in general not possible to utilize only one of them; for a given problem, in general both ϕ_n and $\vec{A}_t$ will be nonzero.

For the special case that $\vec{B} = \vec{\nabla}V$, we have $\vec{\nabla}\times\vec{B} = 0$; furthermore, if V is a solution of the Laplace equation $\vec{\nabla}^2 V = 0$, we have $\vec{\nabla}\cdot\overrightarrow{B} = 0$. Thus in this case, all the volume integral terms vanish, and $\phi_n\left(\vec{x}\right)$ and $\vec{A}_t\left(\vec{x}\right)$ are completely determined from the normal and the tangential components of $\vec{B}$ on the surface $\partial\Omega$ via

$$\begin{aligned}\phi_n\left(\vec{x}\right) &= \frac{1}{4\pi}\int_{\partial\Omega} \frac{\vec{n}\left(\vec{x}_s\right)\cdot\overrightarrow{B}\left(\vec{x}_s\right)}{\left|\vec{x}-\vec{x}_s\right|}ds \\ \vec{A}_t\left(\vec{x}\right) &= -\frac{1}{4\pi}\int_{\partial\Omega} \frac{\vec{n}\left(\vec{x}_s\right)\times\overrightarrow{B}\left(\vec{x}_s\right)}{\left|\vec{x}-\vec{x}_s\right|}ds\end{aligned}$$

For any point within the volume Ω, the scalar and vector potentials and consequently the solution of the Laplace equation depend only on the field on the surface $\partial\Omega$.

Using the fact that if $\vec{x} \neq \vec{x}_s$, we have $\vec{\nabla}\left(1/\left|\vec{x}-\vec{x}_s\right|\right) = -\left(\vec{x}-\vec{x}_s\right)/\left|\vec{x}-\vec{x}_s\right|^3$, and similar relationships, it is possible to explicitly obtain the gradient of the scalar potential, and with some more work the curl of the vector potential; the results have the explicit form

$$\begin{aligned}&\vec{\nabla}\phi_n\left(\vec{x}\right) \\ &= -\frac{1}{4\pi}\int_{\partial\Omega} \frac{\left(\vec{x}-\vec{x}_s\right)\left(\vec{n}\left(\vec{x}_s\right)\cdot\overrightarrow{B}\left(\vec{x}_s\right)\right)}{\left|\vec{x}-\vec{x}_s\right|^3}ds \qquad (3)\end{aligned}$$

$$\begin{aligned}&\vec{\nabla}\times\vec{A}_t\left(\vec{x}\right) \\ &= \frac{1}{4\pi}\int_{\partial\Omega} \frac{\left(\vec{x}-\vec{x}_s\right)\times\left(\vec{n}\left(\vec{x}_s\right)\times\overrightarrow{B}\left(\vec{x}_s\right)\right)}{\left|\vec{x}-\vec{x}_s\right|^3}ds \qquad (4)\end{aligned}$$

From eq.(2) we know that the field inside the volume of interest is just a sum of the irrotational(eq.(3)) and the solenoidal(eq.(4)) part. This is then the solution for the magnetic field as surface integrals. But to numerically integrate the kernel and get the validated solution as the local Taylor model we need a specialized numerical scheme. In the next section we introduce one such scheme based on the Taylor models of the code COSY Infinity[4, 6]. We quickly introduce the definition of the Taylor model and discuss briefly the anti-derivation operation on the

Taylor models which will be extensively used in implementation of the scheme. We then proceed to explain the numerical scheme to perform the surface integration.

2.2 Solution of the Helmholtz Problem using Taylor Models

In the following, we develop a validated method based on Taylor model methods to determine sharp enclosures of the field $\vec{B}$ and the potential ψ utilizing the Helmholtz method.

Definition (Taylor Model) Let $f : D \subset R^v \longrightarrow R$ be a function that is $(n+1)$ times continuously partially differentiable on an open set containing the v-dimensional domain D. Let x_0 be a point in D and P the n-th order Taylor polynomial of f around x_0. Let I be an interval such that

$$f(x) \in P(x - x_0) + I \text{ for all } x \in D$$

and that has the property that I scales with the $(n+1)$st power of the width of D. Then we call the pair (P, I) an n-th order Taylor model of f around x_0 on D.

A full theory of Taylor model arithmetic for elementary operations, intrinsic functions, initial value problems and functional inversion problems has been developed; see [9, 10] and references therein. Details about the validated implementation of arithmetic operation in COSY can be found in [13, 10]. For the purposes of the further discussion, one particular "intrinsic" function, the so-called antiderivation, plays an important role. We note that a Taylor model for the integral with respect to variable i of a function f can be obtained from the Taylor model (P, I) of the function by merely integrating the part P_{n-1} of order up to order $n-1$ of the polynomial, and bounding the n-th order into the new remainder bound. Specifically, we have

$\partial_i^{-1}(P, I) =$

$\left(\int_0^{x_i} P_{n-1}(x)\, dx_i, (B(P - P_{n-1}) + I) \cdot (b_i - a_i)\right).$

More details about the implementation of the antiderivation operation can be found in [5].

Utilizing Taylor model arithmetic, the following algorithm now allows to solve the Laplace equation for the Helmholtz problem.

(1) Discretize the surface $\partial\Omega$ into individual surface cells S_i with centers s_i and the volume Ω into volume cells V_j with centers v_j.
(2) Pick a volume cell V_j.
(3) For each surface cell S_i, evaluate the integrands in eq. (3) and (4), the so-called "kernels", in Taylor model arithmetic to obtain a Taylor model representations in BOTH the surface variables of S_i AND the volume variables of V_j, i.e. in a total of five variables.
(4) Use the Taylor model anti-derivation operation twice to perform integration over the surface variables of each cell S_i.
(5) Add up all results to obtain a three dimensional Taylor model enclosing the field $\vec{B}$ over the volume cell V_j.
(6) If a validated enclosure of the potential ψ to $\vec{B}$ over the volume cell V_j is desired, integrate the field $\vec{B}$ over any path using the anti-derivation operation.

As a result, for each of the volume cells V_j, Taylor model enclosures for the fields $\vec{B}$ and potentials ψ are obtained. All the mathematical operations to evaluate these Taylor Models and surface integration are implemented using the Taylor Model tools available in the code COSY Infinity[4, 6].

Apparently the computational expense scales with the product of the number of volume elements and the number of surface elements; of these, the number of volume elements is more significant because of their larger number. In practice one observes that when using high-order Taylor models, a rather small number of volume elements is required, in particular compared to the situation in conventional field solvers discussed above.

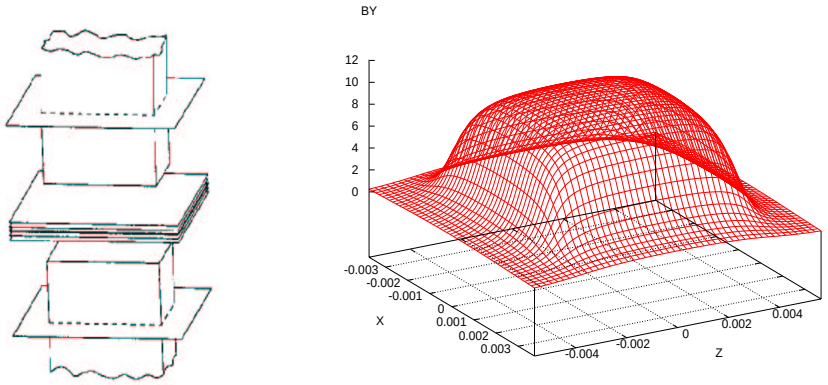

Figure 1: Geometric layout of the bar magnet, consisting of two bars of magnetized material (left), and the magnetic field component B_y on the center plane of the bar magnet (right).

3 An Example: the Bar Magnet

3.1 The Example Field

As a reference problem to study the behavior of the method, we consider the magnetic field of rectangular iron bars of a uniformly magnetized material with inner surfaces ($y = \pm y_0$) parallel to the mid-plane $y = 0$ as shown in fig.1. The geometry of these uniformly magnetized bars, which are assumed to be infinitely extended in the $\pm y$-directions, is defined by: $x_1 \leq x \leq x_2, |y| \geq y_0$, and $z_1 \leq z \leq z_2$. From this bar magnet one can obtain an analytic solution for the magnetic field $\vec{B}(x, y, z)$ - see for example [8, 7, 3] - and the result is given by

$$
\begin{aligned}
B_y(x,y,z) &= \frac{B_0}{4\pi} \sum_{i,j=1}^{2} (-1)^{i+j} \left[\arctan\left(\frac{X_i \cdot Z_j}{Y_+ \cdot R_{ij}^+} \right) \right. \\
&\qquad \left. + \arctan\left(\frac{X_i \cdot Z_j}{Y_- \cdot R_{ij}^-} \right) \right] \\
B_x(x,y,z) &= \frac{B_0}{4\pi} \sum_{i,j=1}^{2} (-1)^{i+j} \left[\ln\left(\frac{Z_j + R_{ij}^-}{Z_j + R_{ij}^+} \right) \right] \\
B_z(x,y,z) &= \frac{B_0}{4\pi} \sum_{i,j=1}^{2} (-1)^{i+j} \left[\ln\left(\frac{X_j + R_{ij}^-}{X_j + R_{ij}^+} \right) \right]
\end{aligned}
\tag{5}
$$

where $X_i = x - x_i, Y_\pm = y_0 \pm y, Z_i = z - z_i$, and $R_\pm = \left(X_i^2 + Y_j^2 + Z_\pm^2 \right)^{\frac{1}{2}}$.

3.1.1 Results and Analysis

As a first step in the analysis of the influence of the discretization of the surface and volume on the result, we study the contributions of the surface elements towards the remainder interval part of the total integral. The volume expansion point is chosen as $\vec{r} = (.1, .1, .1)$, and the size of the volume box around it is chosen zero. Thus after the surface integration, the polynomial part of the dependence on volume vanishes except for the constant term, and the accuracy is only limited by the width of the surface element, which after integration over the surface variables influences the width of the remainder bound. We plot the width of the remainder interval versus surface element length for the scalar potential Fig.2. The center of the surface element is chosen as $\vec{r}_s = (.034, .011, .5)$. It is observed that for high orders, the method quickly reaches an accuracy of around 10^{-16} for about 2^5 surface subdivisions, which correspond to about $2^{10} \approx 1000$ surface element cells per surface. Under the assumption that each of these surface cells brings a similar contribution, the accuracy due to the surface discretization will be in the range of approximately $6 \cdot 1000 \cdot 10^{-16} < 10^{-12}$.

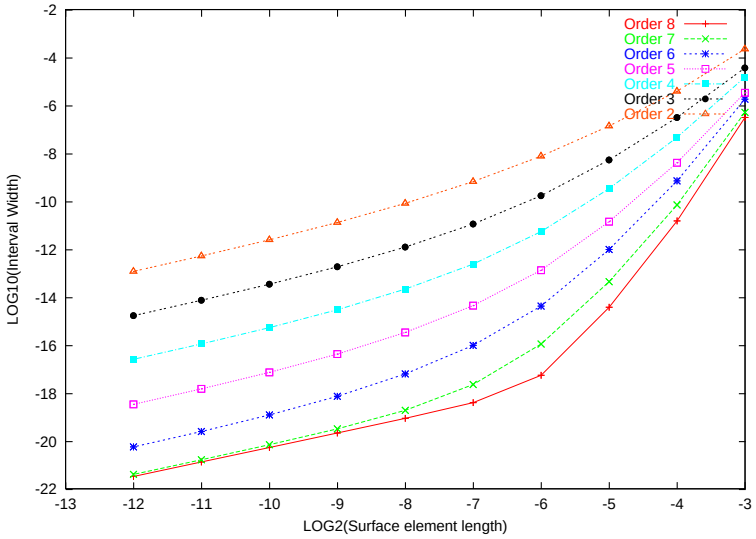

Figure 2: Remainder interval width versus surface element length for integration over a single surface element and vanishing volume size.

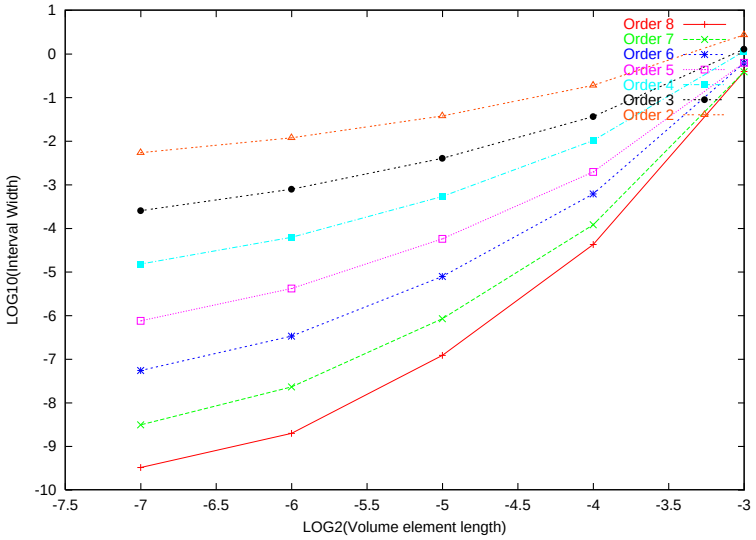

Figure 3: Remainder interval width vs length of volume element for y component of the magnetic field.

We now study the dependency of the polynomial part and width of the remainder interval of the magnetic field on the volume element length. In all these plots the surface element length is kept fixed at 1/128. Figure 3 shows the remainder interval width for the y component of the magnetic field versus volume element lengths for different orders of computation. The other components of the magnetic field exhibit a similar behavior.

We see that a validated accuracy in the range of 10^{-4} can be achieved for a volume element width of around 10^{-1}, corresponding to a total of around 1000 volume elements. This number compares very favorably to the above-mentioned numbers for

the commercial code TOSCA [1, 2]. An accuracy in the range of 10^{-7} can be achieved for a width of around $10^{-1.4}$, corresponding to a total of around $200,000$ volume elements.

Overall, we see that the method of simultaneous surface and volume expansion of the Helmholtz integrals leads to validated tools for the solutions of ODEs which when executed in Taylor model arithmetic can lead to very sharp enclosures. It is obvious that the method can be generalized to other surface-integral based approaches to the solution of PDEs.

References:

[1] The TOSCA reference manual. Technical report, Vector Fields Limited, 24 Bankside, Kidlington, Oxford, OX5 1JE, England.

[2] The TOSCA user guide. Technical report, Vector Fields Limited, 24 Bankside, Kidlington, Oxford, OX5 1JE, England.

[3] M. Berz. *Modern Map Methods in Particle Beam Physics*. Academic Press, San Diego, 1999. Also available at http://bt.pa.msu.edu/pub.

[4] M. Berz, J. Hoefkens, and K. Makino. COSY INFINITY Version 8.1 - programming manual. Technical Report MSUHEP-20703, Department of Physics and Astronomy, Michigan State University, East Lansing, MI 48824, 2002. See also http://cosy.pa.msu.edu.

[5] M. Berz and K. Makino. Verified integration of ODEs and flows using differential algebraic methods on high-order Taylor models. *Reliable Computing*, 4(4):361–369, 1998.

[6] M. Berz and K. Makino. COSY INFINITY Version 8.1 - user's guide and reference manual. Technical Report MSUHEP-20704, Department of Physics and Astronomy, Michigan State University, East Lansing, MI 48824, 2002. See also http://cosy.pa.msu.edu.

[7] R. Degenhardt and M. Berz. High accuracy description of the fringe field in particle spectrographs. *Nuclear Instruments and Methods*, A427:151–156, 1999.

[8] M. M. Gordon and T. Taivassalo. The z^4 orbit code and the focusing bar fields used in beam extraction calculations for superconducting cyclotrons. *Nuclear Instruments and Methods*, 247:423, 1986.

[9] K. Makino. *Rigorous Analysis of Nonlinear Motion in Particle Accelerators*. PhD thesis, Michigan State University, East Lansing, Michigan, USA, 1998. Also MSUCL-1093.

[10] K. Makino and M. Berz. Taylor models and other validated functional inclusion methods. *International Journal of Pure and Applied Mathematics*, 6,3:239–316, 2003. http://bt.pa.msu.edu/pub.

[11] P. M. Morse and H. Feshbach. *Methods of Theoretical Physics, Part I and II*. 1953.

[12] P.L.Walstrom. Soft-edged magnet models for higher-order beam-optics map codes. *Nucl. Instrum. Meth.*, A519, Issues 1-2:216–221, 2004.

[13] N. Revol, K. Makino, and M. Berz. Taylor models and floating-point arithmetic: Proof that arithmetic operations are validated in COSY. *Journal of Logic and Algebraic Programming*, in print, 2004. University of Lyon LIP Report RR 2003-11, MSU Department of Physics Report MSUHEP-30212, http://bt.pa.msu.edu/pub.

[14] M. Venturini, D. Abell, and A. Dragt. Map computation from magnetic field data and application to the LHC high-gradient quadrupoles. *eConf*, C980914:184–188, 1998.

[15] M. Venturini and A. Dragt. Computing transfer maps from magnetic field data. Particle Accelerator Conference (PAC 99), 1999.

[16] M. Venturini and A. J. Dragt. Accurate computation of transfer maps from magnetic field data. *Nucl. Instrum. Meth.*, A427:387–392, 1999.

[17] P. Walstrom, A. Dragt, and T. Stasevich. Computation of charged-particle transfer maps for general fields and geometries using electromagnetic boundary-value data. Particle Accelerator Conference (PAC2001), 2001.

[18] W. Wan. Private communication.